Mat. Res. Soc. Symp. Proc. Vol. 746 © 2003 Materials Research Society 

# Half-Integer Spin Molecular Nanomagnets

David N. Hendrickson,[1*] George Christou,[2*] Wolfgang Wernsdorfer,[3] Stephen O. Hill,[4] Núria Aliaga-Alcade,[2] Sumit Bhaduri,[2] Rachel S. Edwards,[4] Sheila M. J. Aubin,[1] and Ziming Sun[1]

[1]Department of Chemistry and Biochemistry-0358, University of California at San Diego, La Jolla, California 92093-0358, U.S.A.

[2]Department of Chemistry, University of Florida, Gainesville, Florida 32611-7200, U.S.A.

[3]L. Néel-CNRS, BP 166, 25 Avenue des Martyrs, 38042 Grenoble, Cedex 9, France.

[4]Department of Physics, University of Florida, Gainesville, Florida 32611, U.S.A.

## ABSTRACT

Single-molecule magnets (SMM) are molecules that function as single-domain nanomagnets. SMMs have been characterized with a ground-state spin ranging from S = 4 to S = 13. A few SMMs have been identified that have half-integer spin ground states. [Cation][$Mn_{12}O_{12}(O_2CR)_{16}(H_2O)_4$] complexes, where R is some substituent, are SMMs that have either a S = 19/2 or 21/2 ground state. Quantum tunneling of magnetization (QTM) is observed for these half-integer-spin Kramers $[Mn_{12}]^-$ degenerate SMMs in zero external magnetic field, as well as for a class of S = 9/2 $Mn_4$ SMMs. The presence of QTM in zero external field is attributed to a transverse component of a nuclear spin field, dipolar interactions and intermolecular exchange interactions. The Landau-Zener method is used to measure the tunnel splitting as a function of transverse magnetic field for a single crystal of the S = 9/2 SMM [$Mn_4O_3$(OSiMe3)(OAc)3(dbm)3]. Spin parity dependent QTM is established. The effect of a magnetic exchange interaction between two S = 9/2 $Mn_4$ SMMs upon QTM was studied for another compound. The hydrogen bonding and Cl···Cl contacts within a supramolecularly linked $[Mn_4]_2$ dimer lead to a weak antiferromagnetic exchange interaction between the two S = 9/2 SMMs. This interaction causes a shift (exchange bias) from zero field for the magnetic field at which QTM occurs.

## INTRODUCTION

Single-molecule magnets (SMMs) are molecules that function as single-domain magnetic particles which, below their blocking temperature, exhibit the classical macroscale property of a

magnet, namely magnetization hysteresis [1,2]. SMMs owe their properties to a combination of a large ground state spin and an easy-axis-type anisotropy, which give a significant barrier to magnetization relaxation. SMMs thus represent a molecular approach to new nanoscale magnetic materials, offering all the advantages of molecular chemistry (room temperature synthesis, purity, solubility in many solvents, a well defined periphery of organic groups, and a crystalline ensemble of monodisperse units) as well as displaying the superparamagnetism of a mesoscale magnetic particle. They also display quantum tunneling of magnetization (QTM), indicating that they straddle the interface between the classical and quantum regimes [3,4]. SMMs have many potential applications, but these require that their properties be both understood and controlled, particularly QTM. The $Mn_{12}$ SMMs have been the most thoroughly studied of the molecular nanomagnets [5,6]. Various derivatives have been prepared differing in the organic groups [7], and it has been discovered that the magnetic properties (including QTM) can be significantly altered. This is also possible by adding additional electrons, and both the $[Mn_{12}]^-$ (S = 19/2 or 21/2) [8-13] and $[Mn_{12}]^{2-}$ (S = 10) [14,15] versions have been prepared [8-11]. $Mn_4$ SMMs with S = 9/2 have also been extensively studied [16-18].

## EXPERIMENTAL DETAILS

Crystalline samples of the [Cation][$Mn_{12}O_{12}(O_2CR)_{16}(H_2O)_4$] [8] (R = substituent), [$Mn_4O_3(OSiMe_3)(OAc)_3(dbm)_3$] [19] and [$Mn_4O_3Cl_4(O_2CEt)_3(py)_3$] [20] were prepared as reported previously. Magnetization measurements on one salt of the $[Mn_{12}]^-$ SMM were carried out on a few crystals oriented by means of a 5 T field and restrained in eicosane. A Quantum Design SQUID magnetometer was used. All magnetization measurements for the two $Mn_4$ SMMs were carried out on a single crystal using an array of micro-superconducting quantum interference devices (micro-SQUIDs) [21]. The high sensitivity allows one to study single crystals of SMMs on the order of 10-500 μm. The field can be applied in any direction by separately driving three orthogonal coils. Single crystal high-frequency electron paramagnetic resonance (HFEPR) experiments were carried out using a cavity perturbation method, enabling high sensitivity measurements in the range from 20 to 200 GHz; the details of this technique are described elsewhere [22].

## DISCUSSION

Kramers theorem [23] states that no matter how unsymmetric the crystal field is, a molecule possessing an odd number of electrons must have a ground state that is at least doubly degenerate, even in the presence of crystal fields and spin-orbit interactions. A magnetic field is needed to break the symmetry of a half-integer spin SMM and lead to tunneling. There have been several papers [24,25] addressing the fact that a molecule with a half-integer spin (such as S = 19/2) should not exhibit resonant magnetization tunneling in the absence of a magnetic field. For such a molecule, each pair of $\pm m_S$ levels in zero-field exhibits Kramers degeneracy. An S = 19/2 molecule should not be able to tunnel coherently between the $m_S$ = -19/2 and $m_S$ = 19/2 levels, or for that matter, between any $m_S$ and $-m_S$ pair in the absence of a magnetic field.

### $[Mn_{12}]^-$ single-molecule magnets

A few different half-integer SMMs with the composition [Cation][$Mn_{12}O_{12}(O_2CR)_{16}(H_2O)_4$] have been reported [8-13]. The $[Mn_{12}]^-$ SMMs have either a S = 19/2 or a S = 21/2 ground state with axial zero-field splitting ($\hat{DS}_z^2$) where D = -0.4 to -0.6 $cm^{-1}$. The single-crystal X-ray structure of [$PPh_4$][$Mn_{12}O_{12}(O_2CEt)_{16}(H_2O)_4$] (complex 1) has been reported [8]. Five small crystals (3 mm × 0.1 mm × 0.1 mm) of this S=

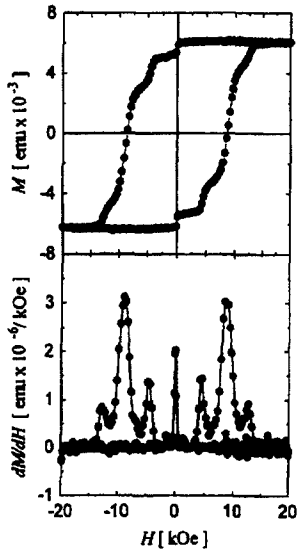


**Figure 1.** The top plot shows the magnetization hysteresis loop measured at 1.85 K for five crystals of [$PPh_4$][$Mn_{12}O_{12}(O_2CEt)_{16}(H_2O)_4$] oriented in an eicosane wax matrix. In the lower plot is shown the first derivative of the magnetization hysteresis loop.

19/2 complex were suspended in eicosane held at 40°C and the suspension introduced into a 5.5 T field, whereupon the five crystals were oriented with their easy axes parallel to the field. The eicosane was cooled to give a wax cube with the five crystals oriented with parallel easy axes. The magnetization versus external magnetic field data exhibit a hysteresis as shown in figure 1.

The sample of complex **1** was first saturated in a field of +2.0 T, and the field was then swept down to -2.0 T and cycled back to +2.0 T. Steps can clearly be seen on the hysteresis loop due to resonant QTM. As the field is decreased, the first step is seen at zero external field. Resonant tunneling occurs because the $-m_S$ levels on the right-hand side of the double well for magnetization reversal have the same energies as the $+m_S$ levels on the left. The most interesting feature on the hysteresis loop is the step seen at zero field. Since complex **1** has a S =

19/2 half-integer spin ground state, it should not be able to tunnel in zero magnetic field. Apparently, the explanation [9] for this step at zero field lies in the fact that several nuclei, particularly the $^{55}Mn$ with I = 5/2, have a nuclear spin. These nuclear spins give rise to a small internal magnetic field inside the molecule. A transverse component of this internal nuclear spin field leads to resonant QTM in zero external field. The suggestion that a nuclear spin field could play this important role was verified [26] by changing iron isotopes in the Fe8 SMM.

The effect of the cation on the properties of $[Mn_{12}]^-$ SMMs has been probed. An early suggestion [10] that a paramagnetic (S = 1/2) cation greatly increased the rate of QTM is apparently incorrect. More detailed studies [12,13] have shown that changing the cation from a diamagnetic one to a paramagnetic one while maintaining the same solid state structure does *not* affect the rate of QTM in the $[Mn_{12}]^-$ SMM.

**[Mn4] single-molecule magnets**

There is a growing family of S = 9/2 SMMs that have the trigonal pyramidal $[Mn^{IV}Mn^{III}_3O_3X]^{6+}$ core where the $X^-$ ligand is variously $Cl^-$, $Br^-$, $N_3^-$, $OH^-$, $MeO^-$, or $Me_3SiO^-$. There are several reasons why these $Mn_4$ complexes are particularly attractive for study as SMMs. Transverse interactions are such that both thermally activated and temperature-independent ground state (*i.e.*, $m_S$ = -9/2 to $m_S$ = 9/2) QTM can be observed for these S = 9/2

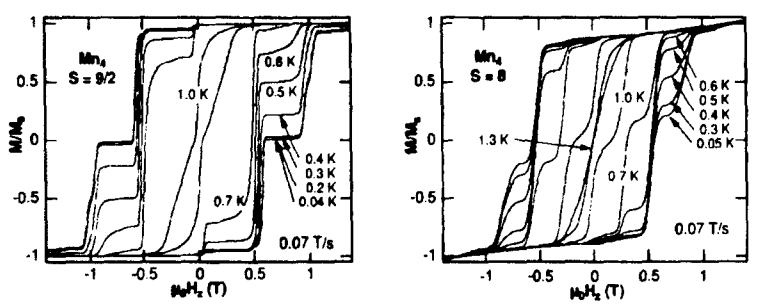


**Figure 2.** Magnetization hysteresis loops for a single crystal of (left plot) $[Mn_4O_3(OSiMe_3)(OAc)_3(dbm)_3]$ (S = 9/2, complex 2) and (right plot) $[Mn_4(OAc)_2(pdmH)_6](ClO_4)_2$ (complex 3) at different temperatures and a constant field sweep rate $dH_Z/dt$ = 0.07 T/s.

SMMs [12,13]. The S = 9/2 $Mn_4$ SMMs have served well to demonstrate for the first time two important phenomena: (1) the spin parity effect for a half-integer SMM; and (2) how magnetic exchange interactions between two SMMs in a crystal can dramatically affect the magnetic field at which resonant QTM occurs.

The spin parity effect was demonstrated [27]for the S = 9/2 SMM $[Mn_4O_3(OSiMe_3)(OAc)_3(dbm)_3]$ (complex **2**) by measuring the tunneling splitting $\Delta_{m,m'}$ as a function of transverse magnetic field. The results for this S = 9/2 SMM were compared to those for two integer spin SMMs, $[Mn_4(OAc)_2(pdmH)_6](ClO_4)_2$ (complex **3**) with S = 8 and the well

known $Fe_8$ SMM with S = 10. Figure 2 shows the magnetization hysteresis loops for single crystals of (left plot) S = 9/2 $Mn_4$ SMM complex **2** and (right plot) S = 8 $Mn_4$ SMM complex **3**. Steps are observed on the hysteresis loops corresponding to resonant QTM. Thus, when the external field is adjusted so that the levels on the left and right side of the potential energy barrier are at equal energy, tunneling occurs and the rate of change of the magnetization increases to give a step. The tunnel splitting for a half-integer SMM is expected to be very sensitive to a transverse magnetic field: a small field will cause the tunnel splitting for a half-integer SMM to change dramatically from zero. On the other hand, the tunnel splitting of an integer spin SMM is expected to change much more gradually in response to a transverse field. The Landau-Zener model [28,29] describes the nonadiabatic transition between two states in a two-level system. When sweeping the longitudinal field $H_Z$ at a constant rate over an avoided energy-level crossing, the tunneling probability P is given in eqn. (1):

$$P_{m,m'} = 1\text{-}\exp\left[\frac{-\pi\Delta^2_{m,m'}}{2\hbar\, g\mu_B |\, m\text{-}m'|\mu_o(dH_z/dt)}\right] \qquad (1)$$

, where m and m´ are the quantum numbers of the avoided level crossing, $dH_Z/dt$ is the constant field sweep rate and $\hbar$ is Planck's constant.

In figure 3 are given the plots of tunnel splitting versus magnitude of transverse magnetic field obtained for single crystals of complexes **2** (S = 9/2), **3** (S = 8) and the $Fe_8$ SMM (S = 10). It is clear that the response of the tunnel splitting with increasing transverse field is much more abrupt for the S = 9/2 complex than for the other two complexes. This is clear evidence for the spin parity effect. In the ideal case, $\Delta = 0$ would be expected for H = 0 in the case of this S = 9/2 SMM, however this is not found because of the influence of environmental degrees of freedom that can induce tunneling. For example, the Mn atoms have a nuclear spin of I = 5/2 and this leads to a small transverse magnetic field that is one form of an "environmental" effect.

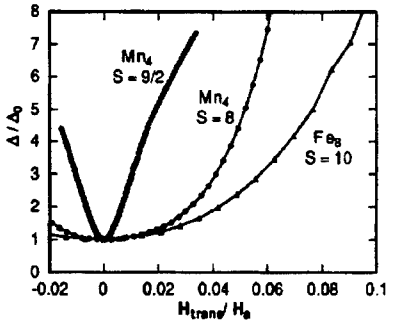


**Figure 3.** Tunnel splitting for three SMMs as a function of transverse field. The tunnel splitting is normalized by $\Delta_0$ = 1.9, 0.94 and 0.28 x $10^{-7}$ K, and the transverse field is normalized by the anisotropy field $H_a = 2DS/g\mu_B$ = 4.6, 5.1 and 4.0 T for complexes 2, 3 and the $Fe_8$ SMM, respectively.

Magnetic exchange-biased QTM can be demonstrated [30] for the S = 9/2 SMM complex **4**, $[Mn_4O_3Cl_4(O_2CEt)_3(py)_3]$. In the crystal there is, in fact, a dimer formed by two of these S = 9/2 $Mn_4$ complexes. Six C-H···Cl hydrogen bonding contacts and one Cl···Cl contact support a weak antiferromagnetic exchange interaction (J = -0.05 K for $\hat{H} = -2K\hat{S}_1\cdot\hat{S}_2$) between the two S = 9/2 moieties in the $[Mn_4]_2$ dimer. As shown in figure 4, this weak intradimer exchange interaction leads to a profound change on the magnetic field at which QTM occurs. The first step for the $[Mn_4]_2$ dimer is seen at -0.33 T after saturation in a field of -1.2 T. Thus, the first step does not occur at zero field, but at -0.33 T; there is an exchange bias. When one S = 9/2 unit in the $[Mn_4]_2$ dimer tunnels from $m_S = -9/2$ to $m_S = 9/2$, the field at which this occurs is shifted from zero to -0.33 T. The field dependencies of all of the energy levels of the $[Mn_4]_2$ dimer can be calculated by diagonalizing the Hamiltonian matrix for the $[Mn_4]_2$ dimer. This explains not only the -0.33 T shift of the first step, but the several

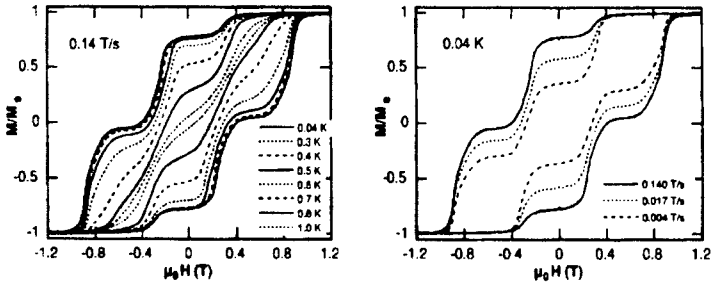


**Figure 4.** Magnetization (M) of $[Mn_4]_2$ (plotted as fraction of maximum value $M_S$) versus applied magnetic field ($\mu_0 H$). The resulting hysteresis loops are shown at different temperatures (left plot) and different field sweep rates (right plot). It is noted that the loops become temperature-independent below about 0.3 K, but are still sweep-rate-dependent owing to resonant QTM between discrete energy levels of the $[Mn_4]_2$ dimer.

other step features seen for this complex.

High-frequency EPR spectra obtained for the $[Mn_4]_2$ dimeric complex definitively confirm the above model for exchange biasing of QTM. The effective spin Hamiltonian for an **isolated** S = 9/2 SMM can be written as in eqn. (2):

$$\hat{H}_i = D\hat{S}_{zi}^2 + (E\hat{S}_{zi}^2 - \hat{S}_{yi}^2) + g\mu_B\hat{B}\cdot\hat{S}_i + \hat{O}_4 + \hat{H}_i' \qquad (2)$$

The first two terms represent the axial and rhombic zero-field interactions, respectively and the third term is the Zeeman interaction. The fourth term gauges fourth order zero-field interactions, whereas the last term $\hat{H}_i'$ describes additional perturbations attributed to disorder, intermolecular

dipolar and exchange interactions. For the $[Mn4]_2$ dimer the magnetic exchange interaction $-2J\hat{S}_1\cdot\hat{S}_2$ couples two S = 9/2 units, each with their own Hamiltonian operators $\hat{H}_1$ and $\hat{H}_2$ to give for the dimer eqn. (3):

$$\hat{H} = \hat{H}_1 + \hat{H}_2 - 2J\hat{S}_1\cdot\hat{S}_2 \qquad (3)$$

where $\hat{H}_1$ and $\hat{H}_2$ are given by eqn. (2). For the S = 9/2 Mn4 unit there are (2S+1) energy levels; for the $[Mn4]_2$ dimer there are (2S+1)x(2S+1) levels. Antiferromagnetic coupling in the $[Mn4]_2$ dimer gives a $S_{total}$ = 0 ground state that is degenerate: (9/2, -9/2) and (-9/2, 9/2) where ($m_{S1}$, $m_{S2}$) specifies the spin state level for the two SMMs in the $[Mn4]_2$ dimer. The energies of the low lying states of the dimer are shown in figure 5 as a function of an external field. It can be seen that when a field is applied parallel to the z axis (easy axis) it can be increased to a value such that there is a crossing of the degenerate (-9/2, 9/2) (9/2, -9/2) levels and the (-9/2, -9/2) level, thereby changing the ground state. Due to the exchange bias, the transition for one Mn4 unit depends on the state of the other Mn4 unit. Thus, the lowest-energy

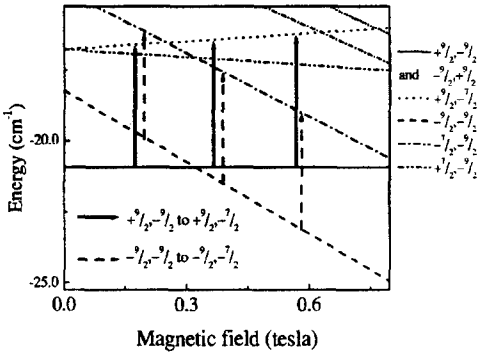


**Figure 5.** The low lying two-spin energy levels for the $[Mn4]_2$ dimer plotted as a function of magnetic field. The most important levels have been labeled according to the scheme described in the text. The calculations of these levels ignored the transverse terms in eqns. (2) and (3).

transitions from the two ground sates, *i.e.*, (9/2, -9/2) to (9/2, -7/2) and (-9/2, -9/2) to (-9/2, -7/2), have slightly different energies even though they both correspond to the same -9/2 to -7/2 transition for one Mn4 unit.

Since many different frequencies can be employed in the HFEPR experiment, one can tune the ground state transition to the field region where the ground state level crossing occurs in figure 5. As can be seen in figure 6, a pronounced splitting is seen in the lowest-field resonance.

The splitting is due to the different energies of the respective (9/2, -9/2) to (9/2, -7/2) and (-9/2, -9/2) to (-9/2, -7/2) ground state transitions. As will be described in detail in a later publication [31], by following this exchange-bias split resonance through the exchange bias field region (~0.3 T), it is clear in figure 6 that the intensity smoothly transfers from one transition to the

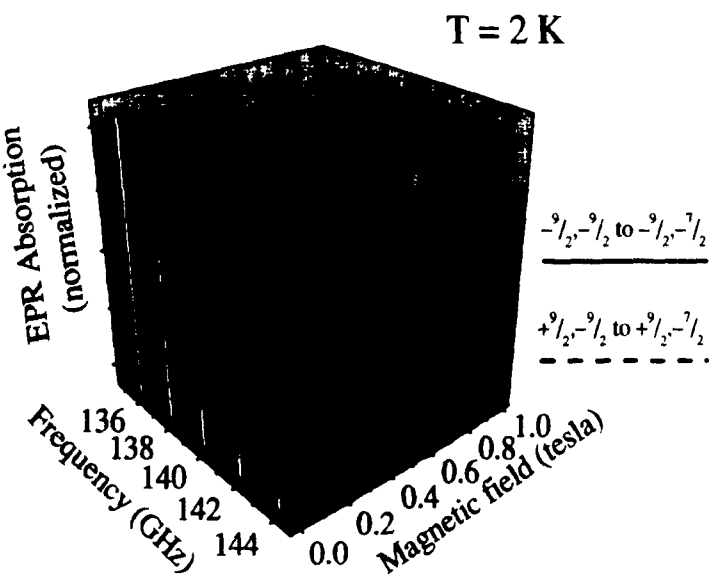


**Figure 6.** A 3D plot of the ground state transitions for the $[Mn_4]_2$ dimer over a narrow field and frequency range. A pronounced splitting is apparent, which is due to the different frequencies of the respective (9/2, -9/2) to (9/2, -7/2) and (-9/2, -9/2) to (-9/2, -7/2) ground state transitions.

other. This clearly establishes a change in the $[Mn_4]_2$ ground state at ~0.3 T. The exchange bias model is substantiated.

A very recent paper [32] has shown that the one-molecule tunnel picture of SMMs is not always sufficient to explain the tunnel transitions observed on magnetization hysteresis loops. Dipolar and weak superexchange interactions between molecules lead to two-molecule tunnel transitions such due to spin-spin cross relaxations.

## CONCLUSIONS

Half-integer ground state single-molecule magnets, such as $[Mn_{12}]^-$ with S = 19/2 or 21/2 and $Mn_4$ with S = 9/2, exhibit resonant quantum tunneling of magnetization in zero external magnetic field. The tunneling in these Kramers degenerate systems in zero external field is due to the presence of nuclear spins that create an internal magnetic field. A micro-SQUID array was used to demonstrate the presence of the spin parity effects for one S = 9/2 $Mn_4$ SMM. The tunnel splitting of this complex responds abruptly to the introduction of a transverse magnetic field, in contrast to the behavior seen for integer spin SMMs. A weak antiferromagnetic interaction between two S = 9/2 $Mn_4$ SMMs in a crystal is shown to bias the magnetic field at which QTM occurs for each S = 9/2 $Mn_4$ unit in the dimer.

## ACKNOWLEDGMENTS

The authors thank the NSF for funding.

## REFERENCES

1. G. Christou, D. Gatteschi, D. N. Hendrickson, and R. Sessoli, MRS Bulletin **25**, 66 (2000).
2. R. Sessoli, H.-L. Tsai, A. R. Schake, S. Wang, J. B. Vincent, K. Folting, D. Gatteschi, G. Christou, and D. N. Hendrickson, J. Am. Chem. Soc. **115**, 1804 (1993).
3. J. R. Friedman, M. P. Sarachik, J. Tejada, and R. Ziolo, Phys. Rev. Lett. **76**, 3830 (1996).
4. L. Thomas, F. Lionti, R. Ballou, D. Gatteschi, R. Sessoli, and B. Barbara, Nature **383**, 145 (1996).
5. M. Soler, P. Artus, K. Folting, J. C. Huffman, D. N. Hendrickson and G. Christou, Inorg. Chem. **40**, 4902 (2001).
6. D. N. Hendrickson, G. Christou, H. Ishimoto, J. Yoo, E. K. Brechin, A. Yamaguchi, E. M. Rumberger, S. M. J. Aubin, Z. Sun and G. Aromi, Polyhedron **20**, 1479 (2001).
7. S. M. J. Aubin, Z. Sun, H. J. Eppley, E. M. Rumberger, I. A. Guzei, K. Folting, P. K. Gantzel, A. L. Rheingold, G. Christou and D. N. Hendrickson, Inorg. Chem. **40**, 2127 (2001).
8. H. J. Eppley, H.-L. Tsai, N. de Vries, K. Folting, G. Christou and D. N. Hendrickson, J. Am. Chem. Soc. **117**, 301 (1995).
9. S. M. J. Aubin, S. Spagna, H. J. Eppley, R. E. Sager, G. Christou and D. N. Hendrickson, J. Chem. Soc., Chem. Commun. 803 (1998).
10. K. Takeda and K. Awaga, Phys. Rev. B **56**, 14560 (1997).
11. S. M. J. Aubin, Z. Sun, L. Pardi, J. Krzystek, K. Folting, L.-C. Brunel, A. L. Rheingold, G. Christou and D. N. Hendrickson, Inorg. Chem. **38**, 5329 (1999).
12. T. Kuroda-Sowa, M. Lam, A. L. Rheingold, C. Frommen, W. M. Reiff, M. Nakano, J. Yoo, A. L. Maniero, L.-C. Brunel, G. Christou and D. N. Hendrickson, Inorg. Chem. **40**, 6469 (2001).
13. T. Kuroda-Sowa, M. Nakano, G. Christou and D. N. Hendrickson, Polyhedron **20**, 1529 (2001).
14. M. Soler, S. K. Chandra, D. Ruiz, J. C. Huffman, D. N. Hendrickson and G. Christou, Polyhedron **20**, 1279 (2001).
15. W. Wernsdorfer, M. Soler, G. Christou and D. N. Hendrickson, J. Appl. Phys. **91**, 7146 (2002).

16. S. M. J. Aubin, M. W. Wemple, D. M. Adams, H.-L. Tsai, G. Christou, and D. N. Hendrickson, J. Am. Chem. Soc. **118**, 7746 (1996).
17. S. M. J. Aubin, N. R. Dilley, M. W. Wemple, M. B. Maple, G. Christou and D. N. Hendrickson, J. Am. Chem. Soc. **120**, 839 (1998).
18. S. M. J. Aubin, N. R. Dilley, L. Pardi, J. Krzystek, M. W. Wemple, L.-C. Brunel, M. B. Maple, G. Christou and D. N. Hendrickson, J. Am. Chem. Soc. **120**, 4991 (1998).
19. S. Bhaduri, M. Pink, K. Folting, W. Wernsdorfer, A. Sieber, H. U. Güdel, D. N. Hendrickson, and G. Christou, manuscript in preparation.
20. D. N. Hendrickson, G. Christou, E. A. Schmitt, E. Libby, J. S. Bashkin, S. Wang, H.-L. Tsai, J. B. Vincent, P. D. W. Boyd, J. C. Huffman, K. Folting, Q. Li and W. E. Streib, J. Am. Chem. Soc. **114**, 2455 (1992).
21. W. Wernsdorfer, T. Ohm, C. Sangregorio, R. Sessoli, D. Mailly and C. Paulsen, Phys. Rev. Lett. **82**, 3903 (1999).
22. M. Mola, S. O. Hill, P. Goy and M. Gross, Rev. Sci. Inst. **71**, 186 (2000).
23. H. A. Kramers, Proc. R. Acad. Sci. Amsterdam **33**, 959 (1930).
24. D. Loss, D. P. Di Vincenzo, G. Grinstein, D. Awschalom and J. F. Smyth, Physica B **189**, 189 (1993).
25. D. P. Di Vincenzo, Physica B **197**, 109 (1994).
26. W. Wernsdorfer, A. Caneschi, R. Sessoli, D. Gatteschi, A. Corina, V. Villar and C. Paulsen, Phys. Rev. Lett. **84**, 2965 (2000).
27. W. Wernsdorfer, S. Bhaduri, C. Boskovic, G. Christou and D. N. Hendrickson, Phys. Rev. B **65**, 180403 (2002).
28. L. Landau, Phys. Z. Sorvjetunion **2**, 46 (1932).
29. C. Zener, Proc. R. Soc. London, Ser. A **137**, 696 (1932).
30. W. Wernsdorfer, N. Aliaga-Alcalde, D. N. Hendrickson and G. Christou, Nature (London) **416**, 406 (2002).
31. R. S. Edwards, S. Hill, S. Bhaduri, N. Aliaga-Alcalde, E. Bolin, S. Maccagnano, G. Christou and D. N. Hendrickson, in preparation.
32. W. Wernsdorfer, S. Bhaduri, R. Tiron, D. N. Hendrickson and G. Christou, Phys. Rev. Lett. **89**, 197201-1 (2002).